

Purdue University Purdue e-Pubs

International Refrigeration and Air Conditioning
Conference

School of Mechanical Engineering

2018

Small, High-Speed, Oil-Free Radial Turbo-compressors for Cooling Applications: Refrigerant Selection

Konstantinos Kontomaris

Chemours Fluorochemicals, Wilmington, Delaware, United States of America, konstantinos.kontomaris@chemours.com

Cordin Arpagaus

NTB University of Applied Sciences of Technology Buchs, Switzerland, cordin.arpagaus@ntb.ch

Stefan Bertsch

Interstate University of Applied Sciences of Technology Buchs, Institute for Energy-Systems IES, Switzerland, stefan.bertsch@ntb.ch

Jürg Schiffmann

Laboratory for Applied Mechanical Design, Ecole Polytechnique Fédérale de Lausanne, jurg.schiffmann@epfl.ch

Follow this and additional works at: <https://docs.lib.purdue.edu/iracc>

Kontomaris, Konstantinos; Arpagaus, Cordin; Bertsch, Stefan; and Schiffmann, Jürg, "Small, High-Speed, Oil-Free Radial Turbo-compressors for Cooling Applications: Refrigerant Selection" (2018). *International Refrigeration and Air Conditioning Conference*. Paper 1946.

<https://docs.lib.purdue.edu/iracc/1946>

This document has been made available through Purdue e-Pubs, a service of the Purdue University Libraries. Please contact epubs@purdue.edu for additional information.

Complete proceedings may be acquired in print and on CD-ROM directly from the Ray W. Herrick Laboratories at <https://engineering.purdue.edu/Herrick/Events/orderlit.html>

Small, High-Speed, Oil-Free Radial Turbo-compressors for Cooling Applications: Refrigerant Selection

Konstantinos (Kostas) KONTOMARIS^{1*}, Cordin ARPAGAU², Stefan S. BERTSCH²,
Jürg SCHIFFMANN³

¹Chemours, Fluorochemicals R&D,
Wilmington, Delaware, USA
konstantinos.kontomaris@chemours.com

²NTB University of Applied Sciences of Technology, Institute for Energy Systems,
Buchs, Switzerland
cordin.arpagaus@ntb.ch; stefan.bertsch@ntb.ch

³EPFL, Laboratory for Applied Mechanical Design,
Neuchâtel, Switzerland
jurg.schiffmann@epfl.ch

* Corresponding Author

ABSTRACT

Emerging energy-efficient, oil-free radial centrifugal compressors seem promising for small to mid-capacity air conditioning and refrigeration applications. Compressor design must balance trade-offs among impeller diameter, bearing type, and refrigerant selection. This paper guides refrigerant selection for single-stage systems delivering 10-250 kW_{therm} of cooling at a representative evaporating temperature of 0 °C. The viable oil-free bearing types, the impeller diameter for maximum compressor efficiency and the resulting system efficiency were determined for a set of representative refrigerants with normal boiling temperatures ranging from -51.7 °C to +49 °C. For residential scale cooling systems, low pressure refrigerants enable high energy efficiency with small size, high-speed centrifugal compressors and vapor-lubricated bearings. For commercial scale cooling systems, medium pressure refrigerants enable high energy efficiency with reasonable size, high-speed centrifugal compressors and vapor-lubricated bearings. For commercial scale cooling systems, low pressure refrigerants enable higher energy efficiency with larger size, high-speed centrifugal compressors and magnetic bearings compared to medium pressure refrigerants with vapor-lubricated bearings. The preferred refrigerant enables combinations of system first and operating costs that are attractive for the intended markets, while meeting equipment reliability, operability and other constraints.

INTRODUCTION

Demand for cooling (e.g. residential or commercial air conditioning or medium temperature refrigeration) at cooling capacities up to 100s of kW_{therm} continues to grow as populations and living standards continue to increase around the world. It is primarily met with systems based on the reverse of the classical Rankine cycle, which involves mechanical compression of a refrigerant. Systems with cooling capacities in the 10s of kW_{therm} are typically based on oil-lubricated scroll compressors and high-pressure refrigerants (e.g. R-410A). Systems with cooling capacities in the few 100s of kW_{therm} are typically based on oil-lubricated screw compressors or oil-free centrifugal compressors with active magnetic bearings and medium-pressure refrigerants (e.g. R-134a). Systems with oil-lubricated compressors must ensure adequate lubricant circulation (especially for two-stage systems) so as to prevent: 1) lubricant depletion at the compressor and associated increased wear; and 2) lubricant accumulation in heat

exchangers (especially cold evaporators) and associated reduced rates of heat transfer (especially from enhanced surfaces).

Cooling consumes a significant fraction of the energy consumed globally. Cooling technologies that reduce energy use have been attracting a growing interest motivated by persistent uncertainty in energy prices and increasing public awareness of the geo-political risks and environmental impacts - including climate change and poor air quality - associated with energy use, in general, and fossil energy, in particular. Emerging energy-efficient, oil-free radial centrifugal compressors in combination with low global warming potential (GWP) refrigerants seem promising for applications requiring cooling capacities in the 10s to 100s kW_{therm} range.

Small, High-Speed Centrifugal Compressors: State of the art

Centrifugal compressors, with impeller diameters as small as 10 mm, operating at rotational speeds exceeding 100,000 rpm, are now feasible (e.g. [1-6]). They are assembled with precisely machined components and they are driven directly (i.e. without gears) by efficient high-speed motors. They have impellers suspended through bearings lubricated by refrigerant vapor, without contact with solid surfaces. Thus, they realize high efficiencies and eliminate the well-known disadvantages resulting from the use and management of conventional lubricants in positive-displacement systems.

The technical feasibility of small-scale, oil-free turbo-compressors supported on gas-lubricated bearings for refrigeration applications was clearly demonstrated by Schiffmann and Favrat [1, 2]. A single-stage centrifugal compressor with a tip diameter of 20 mm was tested in R-134a at rotational speeds up to 210 krpm. It achieved pressure ratios exceeding 3.3, while pulling an electric power of 2 kW and measuring isentropic efficiencies up to 80%. Carre et al. [3] presented first results on a two-stage heat pump (flash cycle) driven by a twin-stage centrifugal compressor with a rotor power of 6 kW supported on self-acting gas lubricated bearings. They identified challenges with regards to the control of the cycle. In addition, they suggested the need for variable inlet guide vanes (IGV) on at least one of the stages in order to better control the matching of the two compressor maps. Twin stage centrifugal compressors supported on active magnetic bearings, with an order of magnitude higher power than the power of the machines tested by Schiffmann and Favrat [2] and by Carré et al. [3], are offered by Turbocor. Much larger industrial chillers using turbo-compressors, usually driven by low speed electric motors (50-60Hz) through gear boxes involving classical oil lubricated rolling element bearings or hydrostatic oil bearings, are available from various manufacturers.

Scaling effects on radial compressors

The key challenges related to reduced scale turbo-compressor are: (1) increased frictional losses resulting from the reduced Reynolds numbers and the increased relative surface roughness; (2) increased relative tip clearance, resulting from assembly tolerances; and (3) non-adiabatic operation, since the ratio between the wetted surface and the cross-section increases with reduced scale. While the increase in frictional losses resulting from reduced Re-number is not a main issue with classical working fluids used in refrigeration, the increased tip clearance can reduce the efficiency significantly. Javed et al. [4] introduced design guidelines for the aerodynamic optimization of small-scale radial compressors for organic working fluids. It is suggested that mid- to aft-loaded impeller designs are best suited for reduced-scale radial compressors operated at large relative tip clearances.

Gas-lubricated bearings and active magnetic bearings

Gas-lubricated bearings are categorized either as self-acting (dynamic) or externally pressurized (static). Self-acting bearings generate load capacity and stiffness through the rotation of the shaft, whereas static bearings are fed from a source of pressurized gas and are therefore dependent on auxiliary power. The main advantage of externally pressurized bearings compared to self-acting designs is that they yield load capacity at zero rotor speed. Nonetheless, due to the requirement of pressurized gas, they significantly reduce the net mechanical efficiency and are, therefore, not well suited for applications in the energy domain, where high efficiencies are required to enable short payback. Typical dynamic gas-lubricated bearings are either herringbone grooved journal bearings (HGJBs) [5-7] or foil bearings (FBs) [8, 9]. Grooved bearings are stabilized by the design of shallow viscous pumping grooves, while foil bearings are stabilized mainly by the damping, introduced by the Coulomb friction between the bump and the top foil. Foil bearings offer high tolerances to misalignment errors and large thermal gradients.

Active magnetic bearings levitate the rotor with an actively controlled magnetic field [10]. The bearings require sensors and a controller and are therefore inherently more expensive than gas-lubricated bearings. On the other hand, these bearing types require no fluid for the lubrication and both stiffness and damping can be tuned individually by the controller. However, catcher bearings are required in order to avoid a rotor failure in case of power loss.

Motivation-Objectives

Optimum design of systems with cooling capacities in the range of 10s to a few 100s kW_{therm} with centrifugal compressors remains an open question. It must balance trade-offs among impeller diameter, bearing type, and refrigerant selection, so as to realize combinations of system first and operating costs that are attractive for the intended markets, while complying with equipment reliability and operability requirements and meeting environmental sustainability objectives and safety constraints.

Although refrigerant selection is key in the design of an optimum cooling system using a centrifugal compressor, it has not been systematically explored for, relatively, low cooling capacities. The primary objective of this paper was to guide refrigerant selection for single-stage systems delivering 10-250 kW_{therm} of cooling at a representative evaporating temperature of 0 °C. The viable oil-free bearing types, the impeller diameter for maximum compressor efficiency and the resulting system efficiency (accounting for the effects of refrigerant thermodynamic properties and compressor electro-mechanical efficiency) were determined for a set of representative refrigerants listed in **Table 1**. The effect of refrigerant selection on heat exchanger design, safety and environmental sustainability were not considered.

Table 1. Refrigerants evaluated for, relatively, small centrifugal cooling systems

		HFC-32	R-290 Propane	HFC-134a	R-600a iso-Butane	R-600 Butane	HFC-245fa	R-601a iso-Pentane	R-601 Pentane	cyclo-Pentane
GWP ₁₀₀		675	~20	1430	~20	~20	1030	~20	~20	
NBP	°C	-51.7	-42.1	-26.1	-11.7	-0.5	15.1	27.8	36.1	49
T _{cr}	°C	78.1	96.7	101.1	134.7	152	154	187.2	196.6	238.6
P _{cr}	MPa	5.78	4.25	4.06	3.63	3.8	3.65	3.38	3.37	4.57

3. METHODS

Technological Roadmap

In order to assess the technical feasibility and the limitations of gas bearing supported centrifugal compressors for typical refrigeration applications depending on the cooling capacity and working fluid, the current investigation considers the impeller design to maximize the isentropic efficiency, the effects of scaling on the rotor design for predicting its weight and the preliminary bearing design in order to assess the feasibility in terms of the rotor-dynamic stability and static load capacity. The high-level approach based on first principles has been put in place according to the following steps:

1. Based on a range of cooling capacities (10-250kW), a given working fluid, a classical single-stage heat pump cycle (evaporation, compression, condensation, expansion) and imposed evaporation and condensing temperatures (0°C and 40°C) the specifications for the compressor are obtained in terms of inlet pressure, pressure ratio and mass-flow. Note that the compressor inlet superheat is adjusted in order to avoid wet compression. The properties of the various working fluids are obtained by Refprop [NIST].
2. The duty imposed by the heat pump cycle, cooling power and working fluid allow then to identify the optimal rotor speed and impeller tip diameter to maximize the isentropic compressor stage efficiency based on Balje's design charts [11]. The optimum specific speed, ns, has been set to 0.95, which yields a corresponding specific diameter, ds, of 3.24. Since these charts have been derived from experimental results of large scale machines the efficiency obtained by these pre-design maps are corrected based on the machine Reynolds-number according to work by Casey [12].

3. Based on a rather conservative NDm value of $2.6 \cdot 10^6 \text{ mm} \cdot \text{rpm}$ for the gas lubricated bearings (rotor speed in rpm and bearing diameter in mm), the rotor speed required by the compressor allows to identify the bearing diameter.
4. Imposing a maximum tip speed of the rotor of the electric motor of 180 ms^{-1} allows to calculate its diameter. The length of the motor is calculated based on the empirical electric motor output equation by Miller and by selecting an electromagnetic shear stress τ of $1.8 \cdot 10^4 \text{ Pa}$ [13].
5. In order to assess the rotor weight as a function of the compressor power and working fluid a classical rotor layout has been selected such as represented in **Figure 1**. A length to diameter ratio of 1 for the two journal bearings, a thrust disc with the same diameter as the impeller tip have been selected. Both rotor and impeller are made of a steel alloy in order to calculate its weight. The impeller weight has been scaled based on the centrifugal compressor tested by Schiffmann and Favrat [1] and by Demierre et al. [14, 15].

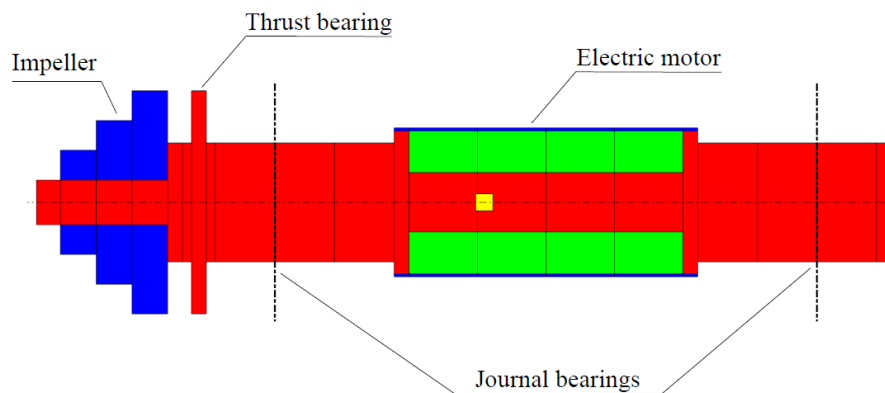


Figure 1: Rotor layout of the gas bearing supported single stage compressor and its dimensions

6. The bearing clearance of the herringbone grooved journal bearings is the main variable governing the rotordynamic stability of high-speed rotors. In this work it has been identified based on work by Fleming and Hamrock [16]. This remarkable paper offers the details of the ideal bearing designs to achieve stable operation while offering a metric for the achievable static load capacity. As a consequence, the bearing clearance has been selected to achieve a sufficiently high stability threshold and the corresponding load capacity.
7. The resulting bearing and electric motor designs are then used to predict the mechanical losses resulting from windage. While the flow can be considered laminar within the bearing fluid film [17], the flow in the airgap of the electric motor is highly turbulent. Correlations introduced by Mack [18] have been implemented to predict the mechanical windage losses of the electric motor. Note that the bearing losses are mainly governed by the fluid viscosity, whereas the windage losses within the motor airgap are dominated by the working fluid density and the viscosity. It has been decided that the bearing-motor unit is exposed to the lowest pressure (evaporation) in order to minimize the mechanical losses.

4. RESULTS

Figure 2 shows the variation of the loads on Herringbone Grooved Journal Bearings (HGJBs) relative to the maximum bearing load capacity predicted at the selected cooling cycle conditions, with system cooling capacity. For cooling capacity of about $10 \text{ kW}_{\text{therm}}$, bearing loads remain within the capability of HGJBs with all refrigerants considered. For progressively higher cooling capacities, bearing loads remain within the capability of HGJBs only with refrigerants which generate progressively higher evaporating pressures. At the maximum cooling capacity

considered, $250 \text{ kW}_{\text{therm}}$, HGJBs remain viable only with the higher-pressure refrigerants among those considered: R-32, propane and R-134a.

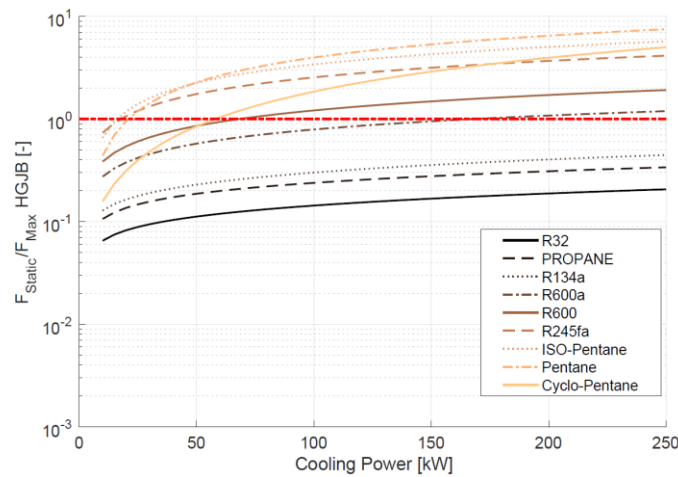


Figure 2: Predicted load on Herringbone Grooved Journal Bearings (HGJB) relative to maximum bearing load capacity versus system cooling capacity

Figure 3 represents the evolution of the bearing compressibility number, which is proportional to the rotor speed and to the square ratio of the bearing radius and the bearing clearance. Increasing compressibility numbers are therefore an indication of increased rotor speed and of reduced clearance ratios. Note that increasingly small clearance ratios are more and more difficult to handle in terms of the manufacturability and yield bearings, which are more prone to seizure due to clearance distortion induced by centrifugal loads and differential thermal expansion. Best engineering practice suggests limiting the bearing compressibility to values of 80. Comparing the bearing compressibility numbers with the optimal rotor speed in **Figure 7** therefore suggests that fluids with lower boiling points are easier to handle than fluids with higher boiling points from a bearing perspective.

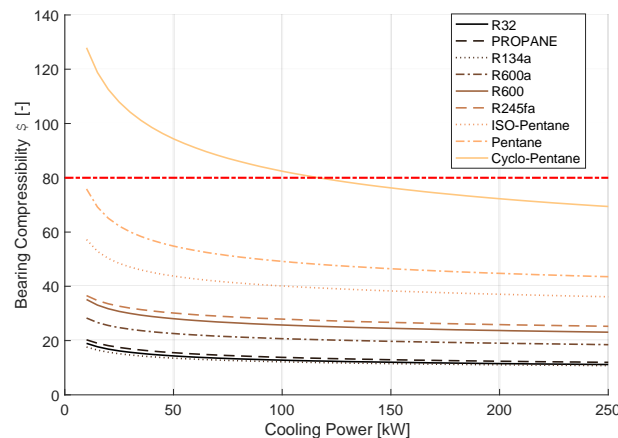


Figure 3: Bearing compressibility number of Herringbone Grooved Journal Bearings (HGJB) versus system cooling capacity

Figure 4 shows the variation of the loads on Foil-gas Bearings (FBs) relative to the maximum bearing load capacity predicted at the selected cooling cycle conditions, with system cooling capacity. For cooling capacities lower than about $20 \text{ kW}_{\text{therm}}$, bearing loads remain within the capability of FBs with all refrigerants considered except for the refrigerant with the lowest vapor pressure at the selected evaporating temperature, namely the cyclo-pentane. For progressively higher cooling capacities, bearing loads remain within the capability of FBs only with refrigerants which generate progressively higher evaporating pressures. At the maximum cooling capacity considered, 250

kW_{therm} , FBs remain viable only with the higher-pressure refrigerants among those considered: R-32, propane, R-134a, R-600a (iso-butane) and R-600 (butane).

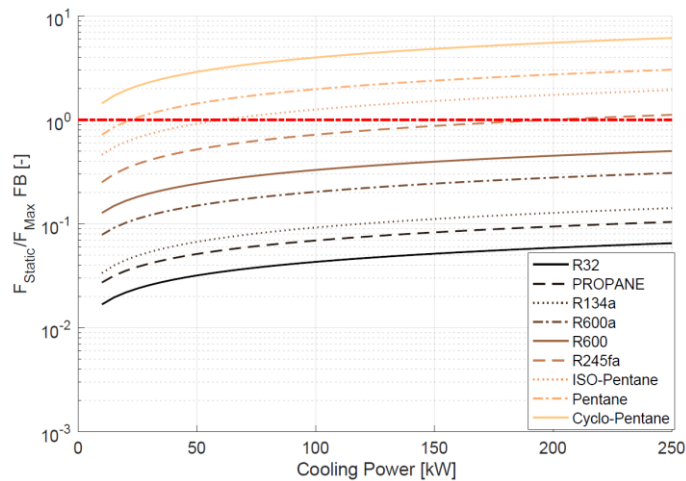


Figure 4: Predicted load on Foil-gas Bearings (FB) relative to the maximum bearing load capacity versus system cooling capacity

Figure 5 shows the variation of the system Coefficient of Performance for cooling, COP_{cool} , predicted at the selected cycle conditions, with system cooling capacity. The COP_{cool} is defined as the ratio of the useful cooling rate (including vapor superheating) delivered by the evaporator and the mechanical power consumed by the compressor. The mechanical power corresponds to the power required to mechanically drive the compressor shaft. This power includes the aerodynamic losses in the impeller as well as the windage losses generated within the journal and thrust bearings as well as within the airgap of the electric motor. The COP_{cool} is steeply lower at lower cooling capacities due to higher compressor energy losses relative to the cooling rate delivered. For example, the COP_{cool} at $10 \text{ kW}_{\text{therm}}$ of cooling capacity is approximately 7.4 - 7.8% (depending on the selected refrigerant) lower than at $50 \text{ kW}_{\text{therm}}$. This drop of efficiency at lower capacities is a consequence of the scaling effect (lower Re-number \rightarrow lower isentropic compressor efficiency) and of the increased mechanical losses. The COP_{cool} at any cooling capacity increases significantly as the normal boiling temperature of the selected refrigerant increases. For example, the COP_{cool} at $10 \text{ kW}_{\text{therm}}$ of cooling capacity increases by 23.8% (from about 3.65 to about 4.52) as the refrigerant normal boiling temperature increases from that of R-32 (-52°C) to that of cyclo-pentane ($+49^\circ\text{C}$). Similarly, the COP_{cool} at $200 \text{ kW}_{\text{therm}}$ of cooling capacity increases by 22.6% (from about 4.16 to about 5.1) as the refrigerant normal boiling temperature increases from that of R-32 (-52°C) to that of cyclo-pentane ($+49^\circ\text{C}$). This is a direct consequence of the lower relative pressure and temperature (relative to the critical point) at which the cycles are operated. Operation at a lower relative temperature yields higher latent evaporation heat and lower vapor quality at the expansion exhaust.

Figure 6 shows the variation of the optimum impeller diameter with system cooling capacity for each selected refrigerant. Smaller impellers are optimum for lower cooling capacities and higher-pressure refrigerants (i.e. refrigerants with higher volumetric cooling capacity). For example, impellers with diameters in the range of about 9.9 - 55 mm (a diameter ratio of up to 5.6, depending on the selected refrigerant) suffice for systems delivering $10 \text{ kW}_{\text{therm}}$ of cooling. Impellers with diameters in the range of about 44 - 210 mm (a diameter ratio of up to 4.8, depending on the selected refrigerant) would be optimum for systems delivering $200 \text{ kW}_{\text{therm}}$ of cooling.

Figure 7 shows the variation of the optimum impeller rotational speed with system cooling capacity for each selected refrigerant. Generally, smaller impellers are rotated at higher speeds, so as to generate tip speeds sufficient to impart the enthalpy of compression needed to lift each refrigerant from its evaporating pressure to its condensing pressure. Even the highest impeller rotational speed of about 650 krpm, required for $10 \text{ kW}_{\text{therm}}$ of cooling with R-32, remains within the capability of available motors.

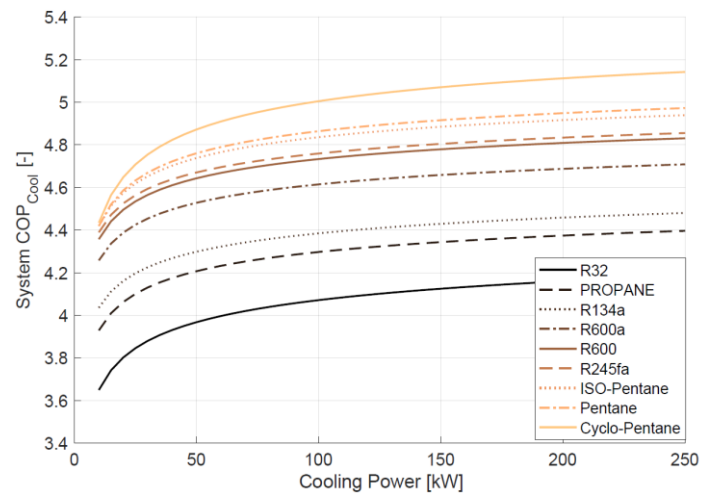


Figure 5: Predicted system COP for cooling versus system cooling capacity

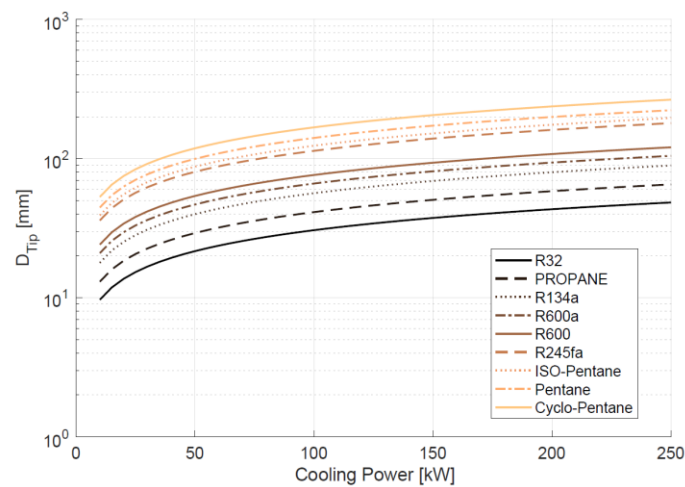


Figure 6: Optimum impeller diameter versus system cooling capacity

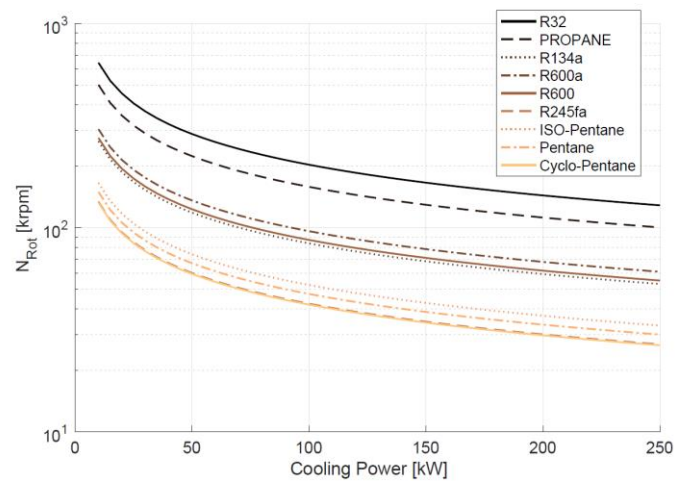


Figure 7: Optimum impeller rotational speed versus system cooling capacity

5. SUMMARY

The primary objective of this paper was to guide refrigerant selection for single-stage systems delivering 10-250 kW_{therm} of cooling at a representative evaporating temperature of 0 °C. The viable oil-free bearing types, the impeller diameter for maximum compressor efficiency and the resulting system efficiency were determined for a set of representative refrigerants with normal boiling temperatures ranging from -52 °C to +49 °C. Results at two selected cooling capacity levels are summarized in **Table 2**.

Table 2: Oil-free bearing types, impeller diameters and COP_{cool} for systems with 10 or 100 kW_{therm} of cooling capacity with R-32, propane, HFC-134a, iso-butane, butane, HFC-245fa, i-pentane, pentane or c-pentane as the refrigerant; (Evaporating Temperature: 0 °C; Condensing Temperature: 40 °C; Liquid subcooling: 0 K; minimum required vapor superheat for dry compression prescribed at each set of cycle conditions)

System Cooling Capacity, kW _{therm}	10	100
Refrigerants for <u>FB Viability</u>	R-32, Propane, HFC-134a, i-Butane, Butane, HFC-245fa, i-Pentane, Pentane	R-32, Propane, HFC-134a, i-Butane, Butane, (HFC-245fa*)
Refrigerants for <u>HGJB Viability</u>	R-32, Propane, HFC-134a, i-Butane, Butane, HFC-245fa, i-Pentane, Pentane, c-Pentane	R-32, Propane, HFC-134a, (i-Butane*)
Impeller <u>Diameter</u> , mm (for maximum compressor efficiency with either FB or HGJB bearings)	9.9 (R-32) - 55 (c-Pentane)	30 (R-32) - 78 (Butane)
System <u>COP_{cooling}</u> (with either FB or HGJB bearings)	3.65 (R-32) - 4.52 (c-Pentane)	4.08 (R-32) - 4.73 (Butane)
Max Impeller <u>Diameter</u> , mm (with magnetic bearings)	55 (c-Pentane)	170 (c-Pentane)
Max System <u>COP_{cooling}</u> (with magnetic bearings)	4.52 (c-Pentane)	5.00 (c-Pentane)

(*) Marginal viability

For residential scale cooling systems (e.g. 10 kW_{therm}) with FB or HGJB gas-lubricated bearings, any of the refrigerants considered can be used without exceeding the bearing load capacity. As the normal boiling temperature of the refrigerant increases from -52 °C to +49 °C, the impeller diameter increases by 5.6 times (from 9.9 mm to 55 mm) but remains relatively small; the system energy efficiency increases by 23.8 % (COP_{cooling} increases from 3.65 to 4.52).

For commercial scale cooling systems (e.g. 100 kW_{therm}) with FB or HGJB gas-lubricated bearings, only the refrigerants with low to medium normal boiling temperatures (or, equivalently, high to medium vapor pressures) can be used: R-32, propane, HFC-134a, iso-butane and butane. The evaporating pressure of the qualifying refrigerants at 0 °C matches or exceeds atmospheric pressure, thus obviating the risk of air-infiltration into non-hermetic equipment with lower pressure refrigerants. As the normal boiling temperature of the refrigerant increases from -52 °C to -0.5 °C, the impeller diameter increases by 2.6 times (from 30 mm to 78 mm) and the system energy efficiency increases by 15.9 % (COP_{cooling} increases from 4.08 to 4.73).

For commercial scale cooling systems (e.g. 100 kW_{therm}) with oil-free magnetic bearings any of the refrigerants considered can be used. Use of the refrigerant with the highest normal boiling temperature (cyclo-pentane) enables a

system energy efficiency ($\text{COP}_{\text{cooling}} = 5.00$) 5.7% higher than the maximum system efficiency feasible with gas-lubricated bearings ($\text{COP}_{\text{cooling}} = 4.73$ with butane). It requires an impeller with a diameter of 170 mm, i.e. 2.2 times larger than the impeller diameter required for highest efficiency with gas-lubricated bearings (78 mm with butane).

The smallest impeller diameter (~10 mm) for the lowest specified cooling capacity (10 kW_{therm}) with the highest pressure (i.e. highest volumetric capacity) refrigerant considered (R-32) remains feasible with available manufacturing methods. The corresponding maximum required impeller rotational speed (~650 krpm) also remains feasible with existing motor technology. Therefore, equipment part manufacturing and motor limitations do not seem to restrict the compressor design space.

6. CONCLUSIONS

- For residential scale cooling systems, low pressure refrigerants enable high energy efficiency with small size, high-speed centrifugal compressors and vapor-lubricated bearings.
- For commercial scale cooling systems, medium pressure refrigerants enable high energy efficiency with reasonable size, high-speed centrifugal compressors and vapor-lubricated bearings.
- For commercial scale cooling systems, low pressure refrigerants enable higher energy efficiency with larger size, high-speed centrifugal compressors and magnetic bearings compared to medium pressure refrigerants with vapor-lubricated bearings.
- Limitations in current methods for manufacturing small compressor parts and in available high-speed motor technology are not restricting the compressor design space.

NOMENCLATURE

NBP	Normal Boiling Point (°C)
GWP	Global Warming Potential
HGJB	Herringbone Grooved Journal Bearing
FB	Foil-gas Bearing
COP_{cool}	Coefficient of Performance for cooling
T_{cr}	critical temperature (°C)
P_{cr}	critical pressure (MPa)

Subscript

cr	critical
therm	thermal

REFERENCES

1. Schiffmann, J. and D. Favrat, *Experimental Investigation of a Direct Driven Radial Compressor for Domestic Heat Pumps*. International Journal of Refrigeration, 2009. **32**(8): p. 1918-1928.
2. Schiffmann, J. and D. Favrat, *Design, experimental investigation and multi-objective optimization of a small-scale radial compressor for heat pump applications*. Energy, 2010. **35**(1): p. 436-450.
3. Carré, J.B., D. Favrat, and J. Schiffmann, *Experimental investigation of a two-stage oil-free domestic Air/Water heat pump prototype powered by an oil-free high-speed twin-stage radial compressor rotating on gas bearings*, in *16th International Refrigeration and Air Conditioning Conference at Purdue* 2016: West Lafayette IN.
4. Javed, A., et al., *Small-scale turbocompressors for wide-range operation with large tip-clearances for a two-stage heat pump concept*. International Journal of Refrigeration-*Revue Internationale Du Froid*, 2016. **69**: p. 285-302.
5. Schiffmann, J. and D. Favrat, *Integrated Design and Optimization of Gas Bearing Supported Rotors*. ASME Journal of Mechanical Design, 2010. **132**(5): p. 051007 1-11.
6. Schiffmann, J., *Enhanced Groove Geometry for Herringbone Grooved Journal Bearings*. Journal of Engineering for Gas Turbines and Power, 2013. **135**(10): p. 102501.

7. E, G. and S. J., *Real-gas effects on aerodynamic bearings*. Tribology International, 2018. **120**: p. 358-368.
8. Agrawal, G.L., *Foil Air/Gas Bearing technology - An Overview*. ASME Paper No. 1997-GT-347, 1997.
9. Schiffmann, J. and Z.S. Spakovszky, *Foil Bearing Design Guidelines for Improved Stability*. ASME Journal of Tribology, 2013. **135**(1): p. 011103.
10. Schweitzer, G., H. Bleuler, and A. Traxler, *Magnetlager*. 1992: Springer-Verlag Berlin.
11. Balje, O.E., *Turbomachines, A guide to Design, Selection and Theory*. 1981: John Wiley & Sons.
12. Casey, M.V., *The Effects of Reynolds Number on the Efficiency of Centrifugal Compressor Stages*. Journal of Engineering for Gas Turbines and Power, 1985. **107**: p. 541-548.
13. Miller, T.J.E., *Switched Reluctance Motors and Their Control*. 1993: Magna Physics Publishing Oxford Science Publication, Oxford UK.
14. Demierre, J., et al., *Experimental investigation of a Thermally Driven Heat Pump based on a double Organic Rankine Cycle and an oil-free Compressor-Turbine Unit*. International Journal of Refrigeration-Revue Internationale Du Froid, 2014. **44**: p. 91-100.
15. Demierre, J., A. Rubino, and J. Schiffmann, *Modeling and Experimental Investigation of an Oil-Free Microcompressor-Turbine Unit for an Organic Rankine Cycle Driven Heat Pump*. Journal of Engineering for Gas Turbines and Power-Transactions of the Asme, 2015. **137**(3).
16. Fleming, D.P. and B.J. Hamrock. *Optimization of self-acting Herringbone Journal Bearings for Maximum Stability*. in *6th International Gas Bearing Symposium*. 1974. Southampton.
17. Cunningham, R.E., D.P. Fleming, and W.J. Anderson, *Experimental Load Capacity and Power Loss of Herringbone Grooved gas Lubricated Journal Bearings*. Journal of Lubrication Technology, 1971. **93**: p. 415-422.
18. Mack, M., *Luftreibungsverluste bei elektrischen Maschinen kleiner Baugröße*, 1967, Universität Stuttgart (FH): Stuttgart.

ACKNOWLEDGEMENT

The authors acknowledge the funding by the Swiss National Science Foundation grant PYAPP2_154278/1 and the Swiss Competence Center for Energy Research SCCER-EIP.